

# INVESTIGATION OF PIPELINE FAILURE IN A THERMAL POWER PLANT'S PROCESS WASTEWATER DISTRIBUTION SYSTEM

## PREISKAVA POŠKODB CEVOVODA V SISTEMU ZA OBDELAVO IN DISTRIBUCIJO ODPADNE VODE TERMOELEKTRARNE

Jakov Batelić<sup>1\*</sup>, Vedrana Špada<sup>2</sup>, Lovro Liverić<sup>3</sup>, Sanja Martinez<sup>4</sup>

<sup>1</sup>HEP Proizvodnja d.o.o. TE Plomin, Plomin luka 50, 52234 Plomin, Croatia

<sup>2</sup>METRIS Materials Research Centre of Region of Istria, Zagrebačka 30, 52100 Pula, Croatia

<sup>3</sup>University of Rijeka Faculty of Engineering, Vukovarska 58, 51000 Rijeka, Croatia

<sup>4</sup>University of Zagreb Faculty of Chemical Engineering and Technology, Marulićev trg 19, 10000 Zagreb, Croatia

*Prejem rokopisa – received: 2020-08-12; sprejem za objavo – accepted for publication: 2020-10-26*

doi:10.17222/mit.2020.159

In this paper, abundant, compacted, dust-like, corrosion scales from the interior of a corrosion-damaged pipeline were analyzed to determine the main reason for leakage and flow damping in the process-wastewater distribution system in the thermal power plant Plomin. The chemical composition, morphology and microbiological activity of the corrosion deposits present on the inner pipe wall were investigated and the physical and chemical analyses of the purified boiler water was made. The results show the presence of iron-related bacteria (IRB) in the corrosion deposits as well as in the distribution system water. XRD analysis shows exclusively magnetite and goethite with no calcium carbonate present in the layers, therefore indicating that no protective carbonate scales, which would protect the pipeline steel, had initially formed. It was concluded that the primary causes of intense corrosion were iron-oxidizing bacteria, that through their metabolism, support the redox cycling process, the formation of large tubercles as well as irregular thinning of the pipeline wall with separated anodic and cathodic areas.

Keywords: pipeline failure, microbiologically influenced corrosion (MIC), process wastewater distribution system, tubercles

V članku avtorji opisujejo analizo obilne, prahu podobne korozijske usedline iz v notranjosti korozijsko poškodovanega cevovoda. Cilj analize je bil določiti glavni razlog za puščanje in dušenje (zmanjšanje) pretoka v cevovodu sistema za distribucijo odpadne vode termoelektrarne Plomin na Hrvaškem. Izvedli so kemijsko in morfološko analizo ter analizo mikrobiološke aktivnosti prisotnih korozijskih usedlin nastalih na notranjih stenah cevi. Izvedli so tudi fizikalno in kemijsko analizo očiščene vode v bojlerju. Rezultati raziskav so pokazali prisotnost bakterij povezanih z železom (IRB, angl.: iron-related bacteria) v korozijskih usedlinah, kakor tudi v sistemu za distribucijo vode. Rentgenska difrakcijska analiza (XRD) je pokazala predvsem prisotnost magnetita in getita. V plasteh pa ni bil prisoten kalcijev karbonat, ki naj bi se tvoril na začetku. Avtorji zato ugotavljajo, da ni prišlo do tvorbe zaščitne plasti, ki bi ščitila jekleni cevovod. V zaključku avtorji poudarjajo, da je primarni vzrok za intenzivno korozijo oksidacija železa zaradi prisotnih bakterij, ki preko svojega metabolizma podpirajo redoks (redukcijsko-oksidacijski) cikel, tvorbo velikih tuberklov (v obliki nabreklih in gomoljev), kakor tudi nepravilno tanjšanje sten cevi v med seboj ločenih anodnih in katodnih področjih.

Ključne besede: poškodbe in odpoved cevovoda, mikrobiološko vplivana korozija, sistem za obdelavo in distribucijo odpadne vode, tuberkli

## 1 INTRODUCTION

Process wastewater is generated as a consequence of the technological process of electricity production. Boiler water is part of process wastewater distribution system and is generated in an auxiliary boiler, stone pulverizers, wash residue of the regenerative air heater, condensate from the boiler area, the bilge pit and the pit of the bunker tract. Given that wastewater is very uneven in quality and quantity, with the purpose of a uniform treatment process, the equalization of wastewater takes place at the thermal power plant Plomin buffer pool with a capacity of 1200 m<sup>3</sup>.<sup>1-3</sup> Further pH stabilization treatments were performed with the help of lime milk by sifting water from the neutralization tank to the sedimentation tank. Through the central pipeline, the wastewater

from the flocculation tank is decanted in the settling tank.<sup>4,5</sup> The clarified wastewater leaves the precipitator through the overflow gutter and goes to the pH control tank where the pH is adjusted with hydrochloric acid and filtered through a sand filter.<sup>6-8</sup> The average inflow of purified wastewater (chemical composition given in **Table 2**) is approximately 5 m<sup>3</sup>/h. The purified water from the sand filter is discharged into accumulation tank, 50 m<sup>3</sup> volume and through the overflow into the surrounding channel. The main purpose of the accumulation tank is to accumulate treated wastewater for rinsing the droplet separator system during the technological process of desulphurization of the flue gases.<sup>7-9</sup> The total average daily water needs for rinsing the droplet separator system 55 m<sup>3</sup>, which means that rinsing can be done entirely using only accumulated wastewater in the thermal power plant Plomin. During daily operations over a period of 6 years, the treated wastewater recovery system

\*Corresponding author's e-mail:  
jbatelic@gmail.com (Jakov Batelić)



**Figure 1:** Appearance of the interior of the investigated steel pressure pipeline

was showing a continuous decrease in the consumption of treated wastewater and an increase in the consumption of raw water for rinsing the droplet separator. By analyzing the values of pressures measured at the beginning and end of the pipeline, it was found that the pressure drop is almost 50 % higher than the constructed values. Therefore, it was concluded that there is significant damping disrupting the pipeline flow and possible leakage. That required more frequent corrective and maintenance actions on the pressure pipeline. With a further visual examination in **Figure 1**, of the cut section of the steel pressure pipeline (DN125, PN 16, total length 820 meters), it was found that deposits were formed on the inner side of the pipe wall. The subjected section of the pressure steel pipe was given a detailed analysis in order to determine the cause of failure.<sup>1-9</sup>

Iron-oxidizing bacteria, also known as metal-depositing microorganisms, is causing microbiologically influenced corrosion (MIC) in many studies.<sup>10-11</sup> MIC is a complex interaction between the environment, the microbial population and the metal substrate.<sup>11-13</sup> It is estimated that microbial activity is causing annually about 20 % of the corrosion damage of metals, of which a significant part is due to aerobic corrosion influenced by iron-oxidizing bacteria (IOB) and anaerobic corrosion influenced by sulfate-reducing bacteria (SRB).<sup>10-12</sup> The reaction of carbon-steel pipes is considered to be a complicated process that is affected by bulk-water quality, including temperature, pH, alkalinity, oxygen concentration and the presence of sulfate and chlorine in the system, etc.<sup>13</sup>

XX Little and Wagner<sup>11</sup> considered that the corrosion occurred in the presence of iron bacteria followed the crevice corrosion mechanism.<sup>11</sup> The role of iron-oxidizing bacteria lies in the formation of condensed oxygen zones and the partition of the metal surface into small anodic sites and large surrounding cathodic area.<sup>11,12</sup>

Moreover, the deposit layers formed by iron-related bacteria could also create condensed oxygen zones and initiate crevice corrosion in water systems containing corrosion inhibitors. The corrosion rate beneath the rust

deposits remains high due to the low penetrability of the corrosion inhibitors and declining of the local oxygen concentration where the site might turn anodic.

During the last decades in the cooling water system of the production industry, SRB and IOB were the most common groups of bacteria on tubercular corrosion and induced microbiologically influenced corrosion in the cooling circuit. They caused poor water quality and equipment clogging, which included flow blockages due to tubercle formation, choking of valves and strainers, pipe punctures and high corrosion rates, resulting in the serious pitting corrosion of carbon-steel equipment.<sup>14</sup>

Despite a large number of research papers reported on the MIC of carbon steels, the quantitative data and information about the real role of the IOB in the MIC process are still not clear, due to the lack of information and evidence of the mechanism describing MIC in water-distribution systems,<sup>10-15</sup> because most of these studies were made in the laboratory. In the present paper, the focus is on understanding the real role of IOB in the MIC-process on the wastewater distribution system of thermal power plant Plomin.

## 2 MATERIALS AND METHODS

### 2.1 Materials

The corrosion-product samples were taken from a section of damaged steel pressure pipeline (total length 820 m, DN125, PN 16). Two main sample categories were visually identified and investigated. One sample unite was named "the black sediment" because it was visually black, and was taken from the bottom and central mass of corrosion scales that was attached to the inner wall of the pipeline. Another sample that was visually brown, was named "the brown sediment" and was taken from the surface of the corrosion scales turned towards the pipeline center. Basic information of the field conditions, as well as the material and year of installation in the power plant, is shown in **Table 1**. The tested wastewater sample came from the same water piping.

**Table 1:** Basic data on the sample of the steel pressure pipeline

User:	HEP-Proizvodnja d.o.o
Plant location:	TE PLOMIN 2, Plomin Luka
Sample dimension:	Pipe $\phi 125 \times 3,6$
Part of installations:	Boiler water pipeline
Working pressure:	7-10 bar
Overheating temperature:	20 °C
Year of construction:	2010.
Pipeline material:	EN St 35.8 (1.0061), DIN 17175

## 2.2 Methods

### 2.2.1 Microbiological analysis of wastewater distribution systems sediment and water

The microbiological test was performed on boiler water taken at the outlet of the system and on the corrosion-products sediment taken from the surface of the pipe. Sulphate-reducing bacteria (SRB) were tested using the Dalynn Biologicals kit, and iron-related bacteria (IRB) using the BTI Products kit. Sargent Welch lead acetate Test Paper and HCl p.a. by Kemika were used for the sulfide presence testing of the bottom, central and top layers of corrosion products.

### 2.2.2 XRD analysis of wastewater distribution systems sediment

Black and brown corrosion products were subjected to X-ray diffraction analysis (PXRD) on a Shimadzu XRD-6000 diffractometer with Cu- $K_{\alpha}$  radiation, with a voltage acceleration of 40 kV and current 30 mA, in the range  $3-83^{\circ} 2\theta$  with a step of  $0.02^{\circ} 2\theta$  and a retention time of 0.6 s. The results are graphically presented as a function of the intensity of diffraction maxima of the diffraction angle on the images appeared.

### 2.2.3 Chemical analysis of water with the calculation of corrosivity indices

Chemical analysis of the wastewater sample was performed in an accredited laboratory for water analysis. Calculation of the Corrosivity Indices was done according to the literature.<sup>16</sup>

**Figure 2:** Control results of: a) IRB-bearing and b) SRB-bearing samples

### 2.2.4 Macro cut of a grinded section of the pipe wall

A macro cut was made from the sample of the steel pipe, on which the corroded wall thickness and its appearance was inspected visually.

## 3 RESULTS AND DISCUSSION

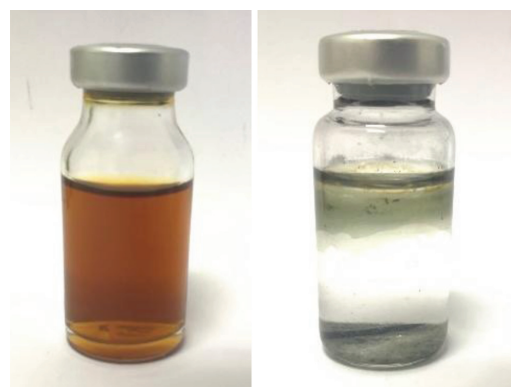
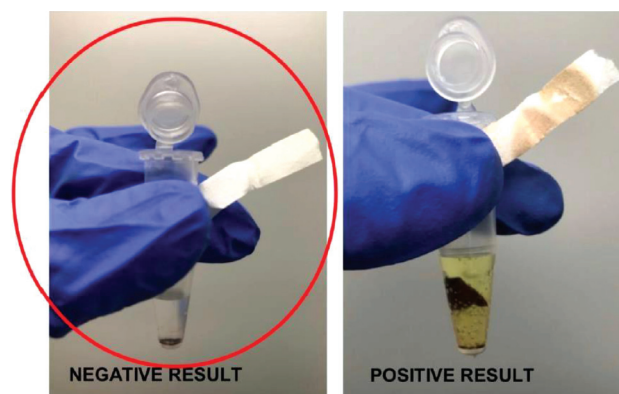
### 3.1 Microbiological analysis of sediments and wastewater

The control results of IRB and SRB-bearing samples are shown in **Figures 2a** and **2b**, respectively. The wastewater and corrosion sediments tests yielded identical results shown in **Figures 3a** and **3b**. Positive results were obtained for IRB and negative for SRB.

The control results of the sulfide analysis for the sulfide-free and sulfide-bearing samples are shown in **Figures 4a** and **4b**, respectively. These were used for a visual assessment of the tested samples.

The results of the sulfide analysis on the central, bottom and top layers of the sediment are shown in **Figure 5**.

Comparison with control samples shows that all three samples were negative, i.e., sulphide-free. Since sulphides are formed as a result of SRB metabolism,<sup>17</sup> this result confirms the previous observation that SRB

**Figure 3:** Results of positive IRB test and negative SRB test, obtained in both wastewater and corrosion product samples**Figure 4:** Control results of a lead acetate paper test on a sulfide-free and a sulfide-bearing sample

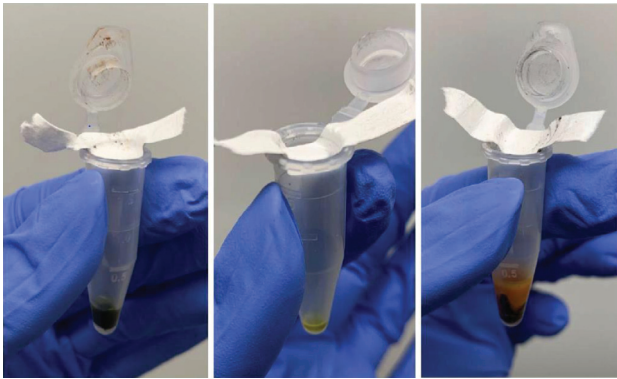


**Figure 5:** Results of three sulphate test made on central, bottom and top layers of the pipeline wall sediment

are not detectable. The microbiological analysis of the sediment samples shows the presence of IRB.

### 3.2 X-ray diffraction analysis

XRD analysis was performed on sediment samples named according to their color, i.e., the black and brown samples. The results are shown in **Figures 6 and 7** as a function of the intensity of the diffraction maxima about the diffraction angle.

The black sediment sample consists of very well crystallized magnetite,  $\text{Fe}_3\text{O}_4$ , ICDD PDF (International Center for Diffraction of the Powder Diffraction File) # 65-3107. No additional diffraction maxima are observed on the diffractogram, thus it can be determined that magnetite is the only crystalline phase in the sample. Moreover, no amorphous halo is observed, so it can be determined that there is no amorphous phase in a larger share.

The diffraction maxima of the brown sediment sample are significantly lower and wider, indicating finer crystallites. No pronounced amorphous halo is observed, although the visual impression may be the opposite due to the low intensities. In this sample, the main crystalline phase is goethite,  $\text{FeO}(\text{OH})$ , ICDD PDF # 81-463, while

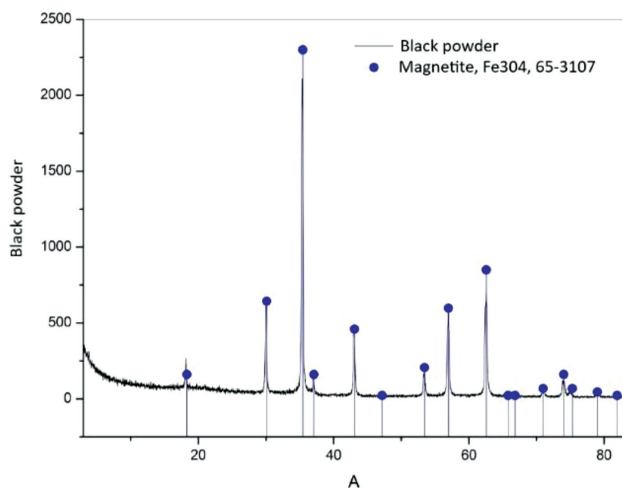


**Figure 6:** XRD analysis of black powder residue

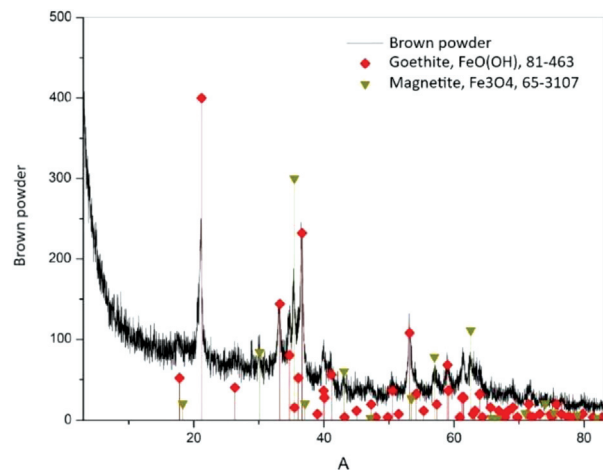


**Figure 7:** XRD analysis of brown powder residue

the secondary phase is magnetite,  $\text{Fe}_3\text{O}_4$ , ICDD PDF # 65-3107. It is not excluded that another crystalline phase is present in a very small proportion in the sample.

The corrosion products are mainly magnetite and to a lesser extent goethite, which is found in a thin surface layer. There is no sulphate-reducing bacteria and sulphides in the composition of the sediment, and it is supported by the appearance of corrosion that indicates this result. Sulphate-reducing bacteria cause very localized damage and the tested sample shows the appearance of general corrosion over the entire surface of the pipe wall.<sup>18,19</sup> The positive test on iron-related bacteria, probably indicates the presence of iron oxidizing bacteria which oxidize  $\text{Fe}^{2+}$ , formed by dissolution of the pipe material, into  $\text{Fe}^{3+}$ .  $\text{Fe}^{3+}$  is an oxidant that significantly promotes the further corrosion of steel. Moreover, redox cyclization probably takes place so that the corrosion process continues. The formation of dense layers of products begins above the anodic site through the accumulation of deposits on the surface.<sup>20</sup> The electrostatic forces gradually strengthen at the location and the surface of the accumulated deposits gradually passes into the cathode. This creates the optimal conditions for the formation of large tubercles.<sup>21</sup>

### 3.4 Macro cut of a grinded section of the pipe wall

A section of the pressure steel pipeline was cut out, freed from loose corrosion products, ground along the profile, to make a macroscopic sample adequate for inspection of the steel pipe thickness, as seen in **Figure 8**.

**Figure 9** shows the inner surface of the pipeline after removal of loose corrosion products. Distinctive, anodic (depressed) and cathodic areas are clearly visible at the surface.

Through a visual inspection it was concluded that the surface was extremely damaged and irregularly thinned. Since the entire surface is equally damaged by corrosion, more and more leaks can be expected to occur on the pipeline over time.

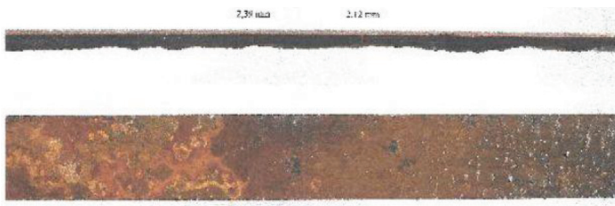


**Figure 8:** Marco cut of the damaged pipe wall after removal of loose corrosion products

### 3.5 Physical and chemical analysis of wastewater with calculation of the corrosivity index

The physicochemical characteristics of the tested wastewater are shown in **Table 2** and the ionic composition is shown in **Table 3**.

The Langelier saturation index (LSI) is defined as:

$$LSI = pH - pH_{sat} \tag{1}$$

where  $pH_{sat}$  is calculated according to:

$$pH_{sat} = (9.3 + A + B) - (C + D) \tag{2}$$

In Equation (2), A depends on the TDS, B depends on the temperature of the water, C depends on the water hardness and D depends on the water alkalinity.

The Larson Skold Index is defined as:

$$L\&Skl = \frac{([Cl^-] + [SO_4^{2-}])}{([HCO_3^-] + [CO_3^{2-}])} \tag{3}$$

where the anion concentrations are presented in **Table 3**.

The calculated values of the Langelier saturation index (LSI) and Larson-Skold index (L&Ski), calculated according to Equations(1-3, as well as their corrosivity assessment are shown in **Table 4**.

According to the Langelier index, the water is non-corrosive and tends to precipitate calcium carbonate. XRD analysis has shown that calcium carbonate is not present in the deposits, therefore indicating that no protective carbonate scales were formed at the pipeline sur-

**Table 2:** Physical and chemical analyses of purified wastewater

Properties	Units	Boiler water – output
Appearance	Descriptive	Transparent
Color	Descriptive	Colorless
Smell	Descriptive	No smell
Temperature	°C	17.4
pH	–	7.4
Electric conductivity	25°C, µS/cm	3079
TDS	mg/L	443.3
Total hardness (Ca + Mg)	mg CaCO <sub>3</sub> mg/L	1665
Water alkalinity (p-, m-)	mg CaCO <sub>3</sub> mg/L	112
Total mineralization	mg/L	2089
Salinity	G NaCl/L	1.33

**Table 3:** Ionic composition of purified wastewater

Ion	Concentration / µL/L	Molar mass /g mol <sup>-1</sup>	Charge	Concentration / meq
Na <sup>+</sup>	25.00	22.99	1	1.0874
K <sup>+</sup>	3.70	39.83	1	0.0929
Ca <sup>2+</sup>	339.00	40.08	2	16.9170
Mg <sup>2+</sup>	199.00	24.31	2	16.3752
NH <sup>4+</sup>	0.58	18.04	1	0.0322
Fe <sup>2+</sup>	0.01	55.85	2	0.0003
toMn <sup>2+</sup>	0.04	54.93	2	0.0014
Sum of cation concentrations				34.4728
Cl <sup>-</sup>	804.00	35.45	-1	22.6779
HCO <sub>3</sub> <sup>-</sup>	137.00	61.02	-1	2.2453
SO <sub>4</sub> <sup>2-</sup>	581.00	96.06	-2	12.0966
Sum of anion concentrations				37.0798
Difference in anion and cation concentration				2.54
Percentage deviation				3.56

**Table 4:** Corrosivity indices of the purified wastewater

Index	Value	Interval	Corrosivity assessment
LSI	0.21	LSI > 0	The water is supersaturated with calcium carbonate and there is a possibility of deposit formation.
L&Skl	15.49	L&Skl > 0.8	Water tends to cause localized corrosion.

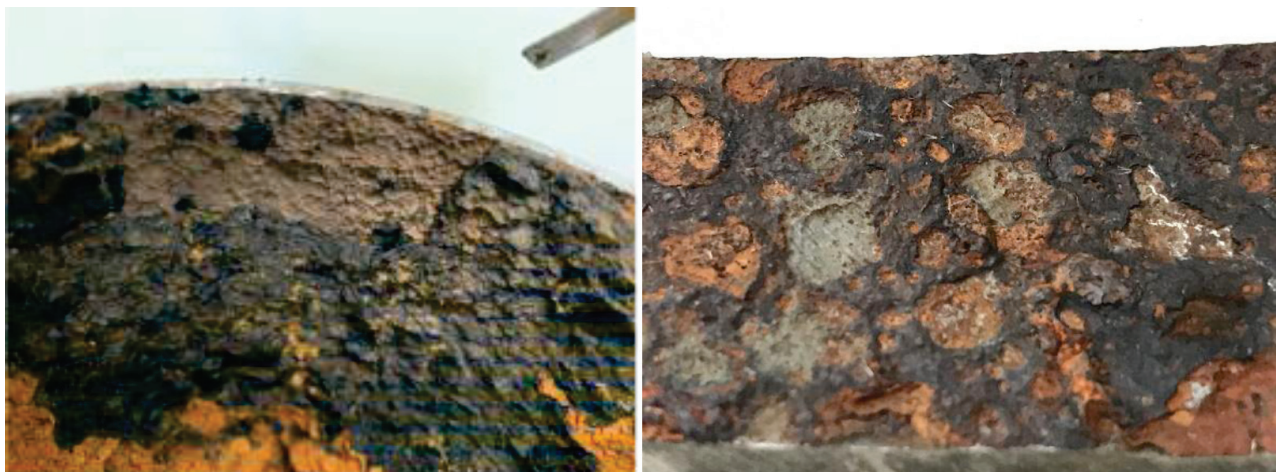


**Figure 9:** Inner surface of the pipe wall after removal of loose corrosion products

face. The Larson Skold Index indicates that wastewater is capable of causing serious localized corrosion. However, from the occurrence of corrosion along the entire wall of the pipeline, it can be concluded that sulphates and chlorides are not decisive corrosion agents, but only corrosion accelerators. The primary causes of the corrosion are likely the iron-oxidizing bacteria, which, in combination with sulphides and chlorides in the wastewater, cause intense corrosion, the formation of abundant, compacted dust-like corrosion products and irregular but general thinning of the pipe wall.

#### 4 CONCLUSIONS

The following conclusions can be drawn:

- Corrosion products are made mostly of compacted dust-like magnetite with a thin surface layer of goethite.
- The presence of IRB was found in the sediment and the distribution system wastewater.
- According to the Langelier index, water should precipitate calcium carbonate, but it has not been identified in the corrosion sediment layer.
- Due to the general appearance of corrosion along the pipeline axes and circumference, sulphates and chlorides, despite the high Larsoon Skold index, are probably not decisive corrosion agents, but only corrosion accelerators.
- The primary causes of corrosion are likely the iron-oxidizing bacteria, which in combination with sulphates and chlorides in the water, cause intense corrosion and the formation of abundant, compacted dust-like corrosion products that are clogging the pipeline.
- The macro sanding of the cut pipe wall revealed that the entire pipe surface, longitudinally and circumferentially, was equally damaged by corrosion, showing irregularities in the form of overlapping wide pits so that over time, more and more leaks can be expected on the pipeline.

#### 5 REFERENCES

- <sup>1</sup> B. Sizirici Yildiz, 18-Water and wastewater treatment: biological processes, *Metropolitan Sustainability*, (2012), 406–428, doi:10.1533/9780857096463.3.406
- <sup>2</sup> M. Živić, A. Galović, J. Avsec, A. Barac, Application of Gas Condensing Boilers in Domestic Heating, *Tehnički vjesnik*, 26 (2019) 3, 681–685, doi:10.17559/TV-20180831125929
- <sup>3</sup> S. Dong, M. A. Page, N. Massalha, A. Hur, K. Hur, K. Bokenkamp, E. D. Wagner, M. J. Plewa, Toxicological Comparison of Water, Wastewaters and Processed Wastewaters, *Environ. Sci. Technol.* 53 (2019) 15, 9139–9147, doi:10.1021/acs.est.9b00827
- <sup>4</sup> A. Ullahab, S. Hussain, A. Wasim, M. Jahanzaib, Development of a decision support system for the selection of wastewater treatment technologies, *Sci Total Environ.* (2020) Aug 20; 731:139158, doi:10.1016/j.scitotenv.2020.139158
- <sup>5</sup> Y. Jin, X. You, M. Ji, On intensive process of quantity and quality improvement of wastewater treatment plant under rainfall conditions, *Desalination and Water Treatment*, 53 (2013) 2, 330–339, doi:10.1080/19443994.2013.841105
- <sup>6</sup> B. Meenakshipriya, K. Saravanan, R. Shanmugam, S. Sathiyavathi, Study of pH System in Common Effluent Treatment Plant, *Modern Applied Science*, 2 (2008) 4, doi:10.5539/mas.v2n4p113
- <sup>7</sup> L. Werncke Vieira, P. Smith Schneider, A. Delavald Marques, T. Haubert Andriotty, Plugin energy penalty model and gypsum production for flue gas desulfurization prediction, *J. Braz. Soc. Mech. Sci.* 42 (2020) 4, doi:10.1007/s40430-020-2209-6
- <sup>8</sup> A. Tijero, A. Moral, A. Blanco, C. Negro, On-line monitorization in a decarbonator-settling tank for water treatment, *WIT Transactions on Ecology and the Environment*, 135 (2010) 12, 311–322, doi:10.2495/WP100271
- <sup>9</sup> Y. Busto, E. W. Palacios, L. M. Rios, L. M. Peralta Suarez, M. Year, Technological proposal for treating wastewater contaminated with nitro aromatic compounds by simulation, *Chemical Engineering Transactions*, 52 (2016) 907–912, doi:10.3303/CET1652152
- <sup>10</sup> H. Ashassi-Sorkhabi, M. Moradi-Haghighi, G. Zarrini, R. Javaherdashti, Corrosion behavior of carbon steel in the presence of two novel iron-oxidizing bacteria isolated from sewage treatment plants, *Biodegradation*, 23 (2012) 69–79, doi:10.1007/s10532-011-9487-8
- <sup>11</sup> Q. I. Beimeng, C. Chongwei, Y. Yixing, Effects of Iron Bacteria on Cast Iron Pipe Corrosion and Water Quality in Water Distribution Systems, *Int. J. Electrochem. Sci.*, 11 (2016) 545–558
- <sup>12</sup> D. Starosvetskya, R. Armonb, J. Yahaloma, J. Starosvetskyb, Pitting corrosion of carbon steel caused by iron bacteria, *International Biodeterioration & Biodegradation*, 47 (2001) 2, 79–87, doi:10.1016/S0964-8305(99)00081-5
- <sup>13</sup> J. Starosvetsky, D. Starosvetsky, R. Armon, Identification of microbiologically influenced corrosion (MIC) in industrial equipment failures, *Engineering Failure Analysis*, 14 (2007) 8, 1500–1511, doi:10.1016/j.engfailanal.2007.01.020
- <sup>14</sup> C. Xua, Y. Zhang, G. Chenga, W. Zhub, Localized corrosion behavior of 316L stainless steel in the presence of sulfate-reducing and iron-oxidizing bacteria, *Materials Science and Engineering A*, 443 (2007) 1–2, 235–241, doi:10.1016/j.msea.2006.08.110
- <sup>15</sup> R. Zuo, T. K. Wood, Inhibiting mild steel corrosion from sulfate-reducing and iron-oxidizing bacteria using gramicidin-S-producing biofilms, *Applied Microbiology and Biotechnology*, 65 (2004) 6, 747–53, doi:10.1007/s00253-004-1651-1
- <sup>16</sup> I. Skoczko, E. Szatylowicz, Treatment Method Assessment of the Impact on the Corrosivity and Aggressiveness for the Boiler Feed Water, *Water* 2019, 11 (2019), 1965, doi:10.3390/w11101965
- <sup>17</sup> J. Kováč, M. Vítězová, I. Kushkevych, Metabolic Activity of Sulfate-Reducing Bacteria from Rodents with Colitis, *Open Med.* (2018) 13, 344–349, doi:10.1515/med-2018-0052
- <sup>18</sup> D. Enning, H. Venzlaff, J. Garrelfs, H. T. Dinh, V. Meyer, K. Mayrhofer, A. W. Hassel, M. Stratmann, F. Widdel, Marine sulfate-reducing bacteria cause serious corrosion of iron under electroconductive biogenic mineral crust, *Environ Microbiol.*, 14 (2012) 7, 1772–1787, doi:10.1111/j.1462-2920.2012.02778.x
- <sup>19</sup> D. Enning, J. Garrelfs, Corrosion of Iron by Sulfate-Reducing Bacteria: New Views of an Old Problem, *Appl Environ Microbiol.* 80 (2014) 4, 1226–1236, doi:10.1128/AEM.02848-13
- <sup>20</sup> N. Eliaz, Corrosion of Metallic Biomaterials: A Review, *Materials (Basel)*, 12 (2019) 3, 407, doi:10.3390/ma12030407
- <sup>21</sup> D. M. F. Santos, C. A. C. Sequeira, J. L. Figueiredo, Hydrogen production by alkaline water electrolysis, *Química Nova*, 36 (2013) 8, 1176–1193, doi:10.1590/S0100-40422013000800017